# Effects of rescaling bilinear interpolant on image interpolation quality

Rukundo, Olivier; Schmidt, Samuel

*Published in:*
Optoelectronic Imaging and Multimedia Technology V

*DOI (link to publication from Publisher):*
10.1117/12.2501549

*Publication date:*
2018

*Document Version*
Publisher's PDF, also known as Version of record

# Effects of rescaling bilinear interpolant on image interpolation quality

Olivier Rukundo, Samuel E. Schmidt

Olivier Rukundo, Samuel E. Schmidt, "Effects of rescaling bilinear interpolant on image interpolation quality," Proc. SPIE 10817, Optoelectronic Imaging and Multimedia Technology V, 1081715 (2 November 2018); doi: 10.1117/12.2501549

SPIE.

Event: SPIE/COS Photonics Asia, 2018, Beijing, China

# Effects of rescaling bilinear interpolant on image interpolation quality

Olivier Rukundo[1a], Samuel E. Schmidt[a]
[a]Department of Health Science and Technology, Fredrik Bajers Vej 7, 9220 Aalborg, Denmark

## ABSTRACT

Rescaling bilinear (RB) interpolant's pixels is a novel image interpolation scheme. In the current study, we investigate the effects on the quality of interpolated images. RB determines the lower and upper bounds using the standard deviation of the four nearest pixels to find the new interval or range that will be used to rescale the bilinear interpolant's pixels. The products of the rescaled-pixels and corresponding distance-based-weights are added to estimate the new pixel value, to be assigned at the empty locations of the destination image. Effects of RB on image interpolation quality were investigated using standard full-reference and non-reference objective image quality metrics, particularly those focusing on interpolated images features and distortion similarities. Furthermore, variance and mean based metrics were also employed to further investigate the effects in terms of contrast and intensity increment or decrement. The Matlab based simulations demonstrated generally superior performances of RB compared to the traditional bilinear (TB) interpolation algorithm. The studied scheme's major drawback was a higher processing time and tendency to rely on the image type and/or specific interpolation scaling ratio to achieve superior performances. Potential applications of rescaling based bilinear interpolation may also include ultrasound scan conversion in cardiac ultrasound, endoscopic ultrasound, etc.

**Keywords:** rescaling bilinear interpolant, image quality, sectored image, image interpolation, standard deviation

## 1. INTRODUCTION

Image interpolation quality can be understood as the image quality after interpolation. Image quality can refer to the level of accuracy in which different imaging systems present the signals that form an image. It can also refer to the weighted combination of the visually significant samples that make an image pleasant or visually artefact-free for observers [1]. Many works on image interpolation kept focusing on the minimization of visual artefacts – by either fitting the interpolation function (i.e. using non-adaptive or single kernel-based interpolation methods) or taking some image samples into account (i.e. using adaptive or edge-directed interpolation methods) [2], [3] – but very few, [10], focused specifically on the role of the spatial distribution of image pixels. For example, in [9], efforts have been made to minimize the relentless image interpolation artefacts by turning the interpolated value into the weighted mean between the pixel value corresponding to the smallest absolute difference and traditional bilinear interpolation value. In [5], a bilinear interpolation optimization method using ant colony algorithm has been introduced to tackle the isotropic assignment of pixels values in the effort to minimize visual artefacts related to such an assignment. In [4], a method based on the statistical selection of the pixel value closest to the traditional bilinear interpolation value has been proposed to efficiently tackle the image edge blurriness problem. In [6], the optimization scheme based on the nearest neighbor algorithm has been proposed with the main objective to improve the speed of the traditional bilinear interpolation algorithm by replacing the traditional bilinear with the nearest interpolation algorithm when the four nearest pixels have the same value. In [8], the author demonstrated the effects of rounding functions on the accuracy of the bilinear interpolation algorithm. In [7], a novel ant colony optimization-based interpolation method which, unlike in [5], uses a global weighting scheme has been proposed to smooth interpolated image edges. In [20], a method that enlarges the interpolation kernel without computing the locations of the nearest pixels has been proposed to create the pixel values leading to less visible interpolation artefacts using extrapolated pixels as well as the nearest four pixels of the traditional bilinear algorithm as the reference. Unlike in above-cited works, in this paper, effects of rescaled image pixels, are investigated in the bilinear interpolation algorithm due to its wide application and particularly in ultrasound imaging systems, in which the bilinear interpolation algorithm is a commonly used method for sectored image scan conversion [21]. For example, in [10], the authors developed a method for interpolating images using contrast enhancement techniques, coupled with additional constraints for the interpolation, to preserve 'sharp edge' information. Here, the studied scheme does not use any image contrast enhancement technique, instead it simply uses the standard deviation of

[1]orukundo@hst.aau.dk; phone 45 4294 8142; www.hst.aau.dk

Optoelectronic Imaging and Multimedia Technology V, edited by Qionghai Dai, Tsutomu Shimura, Proc. of SPIE Vol. 10817, 1081715 · © 2018 SPIE
CCC code: 0277-786X/18/$18 · doi: 10.1117/12.2501549

four nearest pixels to achieve new ranges or intervals on which the source image nearest four pixels can be locally rescaled (before multiplication with the standard distance weighted function) to improve image interpolation quality, in general. This paper is organized as follows: Part 2 gives a brief review of the bilinear interpolation method/algorithm and rescale function. Part 3 introduces the rescaling scheme and demonstrate how the lower and upper bound are determined. Part 4 presents and discusses experimental demonstrations. Part 5 gives the conclusion.

## 2. BILINEAR INTERPOLATION AND RESCALE FUNCTION

The bilinear interpolation is an extension of linear interpolation. It is based on performing interpolation in two directions. As can be seen, in Figure 1's example, the bilinear interpolation algorithm uses four nearest pixels or samples in Equation 1 to estimate or approximate the missing pixel value at $P(x, y)$, [11], [12].

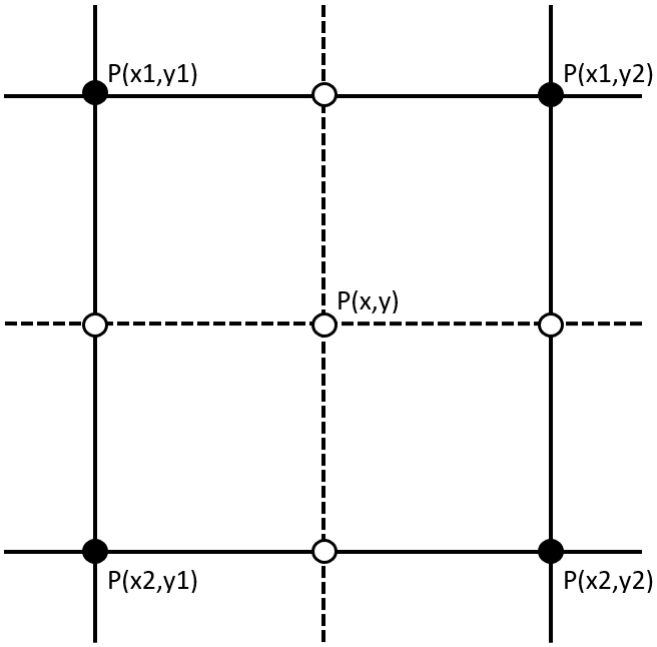


Figure 1: Four nearest pixel samples at the location $(x_1, y_1)$, $(x_1, y_2)$, $(x_2, y_1)$ and $(x_2, y_2)$ of the source image. The 'middle' sample, $P$, represents the pixel value at the location $(x, y)$ of the destination image.

$$P(x,y) = P(x_1,y_1) \times W(x_1,y_1) + P(x_1,y_2) \times W(x_1,y_2) + P(x_2,y_1) \times W(x_2,y_1) + P(x_2,y_2) \times W(x_2,y_2) \qquad (1)$$

where, W, represents the weight (or area) assigned to the pixel samples belonging to the location $(x_1, y_1)$, $(x_1, y_2)$, $(x_2, y_1)$ and $(x_2, y_2)$. For example, $W(x_1, y_1) = (y2 - y) \times (x2 - x)$ with $(x_1 = 1, x_2 = 2)$, $(y_1 = 1, y_2 = 2)$ and $(1 \le x \le 2, 1 \le y \le 2)$. By default, the rescale function rescales elements of an array or vector to the interval $[0,1]$. In other words, suppose we have a vector $V$ containing a certain number of scalar values or elements. In this case, Equation 2 rescales the $[\min(V), \max(V)]$ range to the interval $[0,1]$.

$$R = \left( \frac{V - \min(V)}{\max(V) - \min(V)} \right) \qquad (2)$$

However, when the new interval or range has been specified the rescale function uses Equation 3.

$$R = \left(N\max - N\min\right) \times \left(\frac{V - \min(V)}{\max(V) - \min(V)}\right) + N\min \tag{3}$$

where $[N\min, N\max]$ is the new range or interval specified for rescaling elements of $V$. More details can be found for example in the MATLAB manuals from the R2017b and beyond. In brief, Equation 3 can change the vector $V$'s $[\min(V), \max(V)]$ range to $[N\min, N\max]$ range. By rescaling the vector $V$ elements new elements or values are obtained, which is the key step in this study. How to determine the $[N\min, N\max]$ range is explained in the following part.

## 3. BILINEAR INTERPOLANT PIXELS RESCALING SCHEME

Suppose, we have a row vector $V = [P1\ \ P2\ \ P3\ \ P4]$, consisting of pixel-samples $P(x1, y1)$, $P(x1, y2)$, $P(x2, y1)$ and $P(x2, y2)$, as shown in Figure 1. Now, the question is: How can we determine the lower $\{N\min\}$ and upper bounds $\{N\max\}$ on which the vector $V$ elements can be rescaled without sacrificing image interpolation quality? It is from here, researchers can decide their own way to go because there are possibly many ways to determine such bounds. Therefore, in this paper, the way to go adopted is based on the statistical mean and standard deviation of vector $V$ elements, as shown in Figure 2. The choice of the mean and standard deviation was because, the mean and standard deviation consider every data point or samples, and outliers among those samples, they would positively be part of the solution.

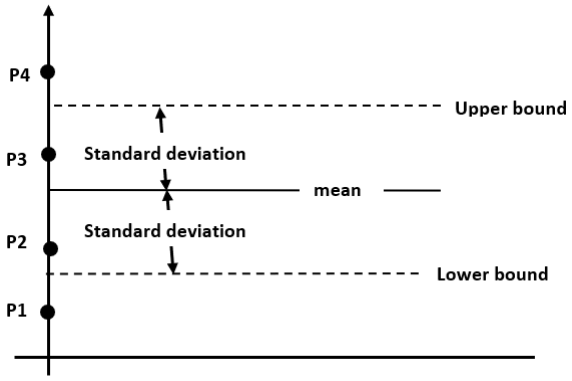


Figure 2: P1, P2, P3, and P4 are elements of the vector V

For a vector $V$ consisting of $N$ scalars (or $N$ pixels), the mean is given by Equation 4.

$$\mu = \frac{1}{N}\sum_{i}^{N} V_i \tag{4}$$

For a vector $V$ consisting of $N$ scalars (or $N$ pixels), the standard deviation (with the normalization factor $N$ instead of $N-1$) is given by Equation 5.

$$\sigma = \sqrt{\frac{1}{N}\sum_{i}^{N}\left(V_i - \mu\right)^2} \tag{5}$$

With Equation 4 and Equation 5, the equivalent of the lower and upper bounds is given in the Equation 6 and Equation 7, respectively.

$$N\min = \mu - \sigma \tag{6}$$

$$N\max = \mu + \sigma \tag{7}$$

Now, replacing Equation 3 into the Equation 1, the interpolated sample is given by Equation 8.

$$P(x,y) = R(x_1,y_1)\times W(x_1,y_1) + R(x_1,y_2)\times W(x_1,y_2) + R(x_2,y_1)\times W(x_2,y_1) + R(x_2,y_2)\times W(x_2,y_2) \tag{8}$$

Table 1 presents a numerical example, showing how the traditional bilinear's Equation 1 and rescaled bilinear's Equation 8 approximates the interpolated value/sample, differently using the same distance weighted function.

Table 1: Numerical examples

| $x_1$ | $x$ | $x_2$ | $y_1$ | $y$ | $y_2$ | $P1$ | $P2$ | $P3$ | $P4$ | Equation (1) | Equation (8) |
|---|---|---|---|---|---|---|---|---|---|---|---|
| 1 | *1* | 2 | 1 | *1* | 2 | 91 | 210 | 162 | 95 | 91.0000 | 82.3190 |
| 1 | *1.25* | 2 | 1 | *1* | 2 | 91 | 210 | 162 | 95 | 120.7500 | 110.9095 |
| 1 | *1.5* | 2 | 1 | *1* | 2 | 91 | 210 | 162 | 95 | 150.5000 | 139.5000 |
| 1 | *1.75* | 2 | 1 | *1* | 2 | 91 | 210 | 162 | 95 | 180.2500 | 168.0905 |
| 1 | *2* | 2 | 1 | *1* | 2 | 91 | 210 | 162 | 95 | 210.0000 | 196.6810 |
| 1 | *1.25* | 2 | 1 | *1.25* | 2 | 91 | 210 | 162 | 95 | 126.8750 | 116.7958 |
| 1 | *1.5* | 2 | 1 | *1.5* | 2 | 91 | 210 | 162 | 95 | 139.5000 | 128.9287 |
| 1 | *1.75* | 2 | 1 | *1.75* | 2 | 91 | 210 | 162 | 95 | 128.8750 | 118.7178 |
| 1 | *2* | 2 | 1 | *2* | 2 | 91 | 210 | 162 | 95 | 95.0000 | 86.1631 |
| 1 | *2* | 2 | 1 | *2* | 2 | 91 | 91 | 91 | 91 | 91.0000 | 91.0000 |
| 1 | *1.5* | 2 | 1 | *1.5* | 2 | 91 | 91 | 91 | 91 | 91.0000 | 91.0000 |

In the following part, we discuss the effects of the rescaled bilinear interpolant's Equation 8 on image interpolation quality.

## 4. EXPERIMENTS AND DISCUSSIONS

The rescaled bilinear interpolation algorithm has been implemented in MATLAB-R2018a. Among many full-reference and non-reference objective image quality metrics available in the literature, [13], [15], [17], we only chose the feature similarity index (FSIM) [16], and Blind/Referenceless Image Spatial Quality Evaluator (BRISQUE) [14], as well as the variance and mean based equations metrics for statistical visual representation, shown in Equation 9 and Equation 10, [18], [19]. The FSIM and BRISQUE metrics have been chosen to quantify features (against a supposedly pristine or reference image) and distortions similarities (in a referenceless way). Here, the aim is to measure how the traditional and rescaled bilinear images can rapidly be evaluated and get the idea of how their output images would have consisted with subjective evaluations. Note that small-sized and some reference images used were inferred using the Microsoft Picture Manager application. Other two metrics, defined in Equation 9 and Equation 10, consisting of variance and mean equations, have been chosen to define the percentage of increment or decrement of contrast and intensity levels (which are also other key image quality indicators) in each algorithm's output image [19], [18].

$$C = \frac{\sigma_{out} - \sigma_{in}}{\sigma_{in}} \tag{9}$$

$$L = \frac{\mu_{out} - \mu_{in}}{\mu_{in}} \tag{10}$$

where, $\sigma_{out}$ and $\mu_{out}$ are the variance and mean of interpolated images, $\sigma_{in}$ and $\mu_{in}$ are the variance and mean of reference images, respectively [19]. Grayscale images, mostly, downloaded from the USC-SIPI Image database have been used as test images. As can be seen, in Table 2, the effects of rescaling the pixels in bilinear interpolation remained comparable in terms of features similarity, except in terms of image distortions. In other words, the FSIM values obtained indicated a very small difference between the traditional and rescaled bilinear algorithms. In some cases, the traditional bilinear generated higher values than a rescaled bilinear algorithm. Here, it is important to note that the higher the FSIM value means the better image quality. Referring only to seven images presented, in Table 2, the rescaled bilinear algorithm demonstrated generally higher values (in bold) than a traditional bilinear algorithm. In Table 3, the BRISQUE scores presented, indicated that the rescaled bilinear algorithm can reduce image interpolation distortions

(such as jaggedness, blurriness, and noise) better than the traditional bilinear algorithm. Here, it is important to note that the smaller BRISQUE score the better visual quality; and that interpolated image must have at least one of the distortions to be scored by the BRISQUE metric.

Table 2: FSIM for rescaled bilinear (RB) and traditional bilinear (TB), Average (AV)

| | Jet | | Lenna | | House | | Cam.man | | Peppers | | Aerial | | Gray | |
|---|---|---|---|---|---|---|---|---|---|---|---|---|---|---|
| | RB | TB | RB | TB | RB | TB | RB | TB | RB | TB | RB | TB | RB | TB |
| 2X | 0.9544 | 0.9561 | 0.9655 | 0.9658 | **0.9698** | 0.9697 | 0.9551 | 0.9553 | 0.9586 | 0.9615 | 0.9263 | 0.9285 | **0.9863** | 0.9857 |
| 3X | 0.9412 | 0.9425 | 0.9478 | 0.9483 | 0.9475 | 0.9475 | 0.9241 | 0.9241 | **0.9541** | 0.9539 | 0.8821 | 0.8826 | **0.9829** | 0.9815 |
| 4X | **0.9116** | 0.9094 | 0.8820 | 0.8880 | 0.8784 | 0.8810 | 0.8446 | 0.8473 | 0.8740 | 0.8837 | 0.8059 | 0.8067 | 0.9642 | 0.9644 |
| 5X | **0.8968** | 0.8919 | **0.9403** | 0.9380 | **0.9280** | 0.9253 | **0.8902** | 0.8849 | **0.9386** | 0.9351 | **0.7648** | 0.7629 | 0.9574 | 0.9580 |
| 6X | **0.8735** | 0.8734 | 0.8634 | 0.8650 | **0.8534** | 0.8508 | **0.8006** | 0.7982 | **0.8679** | 0.8666 | 0.7120 | 0.7151 | 0.9426 | 0.9432 |
| 7X | **0.8553** | 0.8539 | **0.8484** | 0.8478 | **0.8340** | 0.8302 | **0.7788** | 0.7768 | **0.8476** | 0.8459 | 0.6820 | 0.6843 | **0.9365** | 0.9362 |
| 8X | 0.8379 | 0.8399 | 0.8213 | 0.8225 | **0.8045** | 0.8022 | **0.7507** | 0.7485 | 0.8211 | 0.8214 | 0.6339 | 0.6358 | **0.9204** | 0.9193 |
| AV | **0.8959** | 0.8953 | 0.8956 | 0.8965 | **0.8880** | 0.8867 | **0.8492** | 0.8479 | 0.8946 | 0.8955 | 0.7725 | 0.7737 | **0.9558** | 0.9555 |

In Figure 3, the RB algorithm demonstrated a smaller decrement than the TB in terms of contrast at the interpolation ratios used. However, in terms of intensity, the TB algorithm achieved a bigger increment than the RB algorithm only at the interpolation ratio that equals to two.

Table 3: BRISQUE for rescaled bilinear (RB) and traditional bilinear (TB), Average (AV)

| | Jet | | Lenna | | House | | Cam.man | | Peppers | | Aerial | | Gray | |
|---|---|---|---|---|---|---|---|---|---|---|---|---|---|---|
| | RB | TB | RB | TB | RB | TB | RB | TB | RB | TB | RB | TB | RB | TB |
| 2X | 43.854 | 37.011 | **32.291** | 33.342 | 50.299 | 48.506 | 35.585 | 35.332 | 42.322 | 40.336 | 33.620 | 33.425 | 47.185 | 47.107 |
| 3X | **50.225** | 50.735 | **46.301** | 51.184 | 54.311 | 53.574 | **44.973** | 45.534 | 47.461 | 43.474 | 50.692 | 46.060 | 47.156 | 47.372 |
| 4X | 57.980 | 48.892 | **43.894** | 44.966 | **54.721** | 57.188 | **42.261** | 49.620 | 49.724 | 46.617 | 50.395 | 47.416 | 48.491 | 48.557 |
| 5X | **55.768** | 60.216 | **60.091** | 61.572 | 50.489 | 49.569 | **60.477** | 63.210 | **55.364** | 59.435 | **44.134** | 47.474 | 48.229 | 48.254 |
| 6X | **57.019** | 66.957 | **56.885** | 60.296 | **55.024** | 56.069 | 60.962 | 60.302 | **56.250** | 62.200 | **49.488** | 61.253 | 49.367 | 49.101 |
| 7X | **55.361** | 59.816 | **64.119** | 67.129 | **55.123** | 55.749 | **59.851** | 64.317 | **63.048** | 65.722 | 59.289 | 58.688 | 48.290 | 47.824 |
| 8X | **54.484** | 57.732 | **62.640** | 59.654 | **57.331** | 59.713 | **57.434** | 58.727 | 62.155 | 62.126 | **57.824** | 65.925 | 48.108 | 48.952 |
| AV | **53.527** | 54.480 | **52.317** | 54.021 | **53.900** | 54.338 | **51.649** | 53.863 | **53.761** | 54.273 | **49.349** | 51.463 | **48.118** | 48.167 |

In Figure 4, the RB algorithm demonstrated a smaller decrement than the TB in terms of contrast at the interpolation ratios used. However, in terms of intensity, the TB algorithm achieved a bigger increment than the RB algorithm only at the interpolation ratio that equals to two, four, and six.

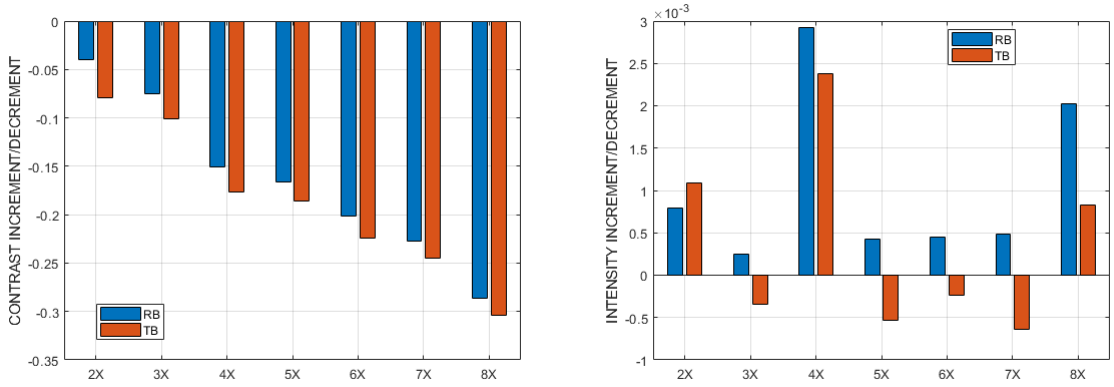


Figure 3: Contrast and Intensity increments or decrements in Jet images interpolated by TB and RB algorithms.

At the interpolation ratio that equals to five and seven, the RB algorithm demonstrated a smaller decrement than the TB in terms of intensity It is important to note that the increment or decrement values shown at the y-axis of figures, represents a certain percentage. For example, if RB algorithm's image has contrast decrement value that equals to -0.035 and intensity increment values that equal to 0.00075, it means that the contrast and intensity levels of RB algorithm's image are -3.5 and 0.075 times less and higher than the reference image, respectively. Here, the negative sign denotes the decrement while the positive sign denotes the increment. In Figure 5, the RB algorithm demonstrated a smaller decrement than the TB algorithm in terms of contrast at the interpolation ratios used.

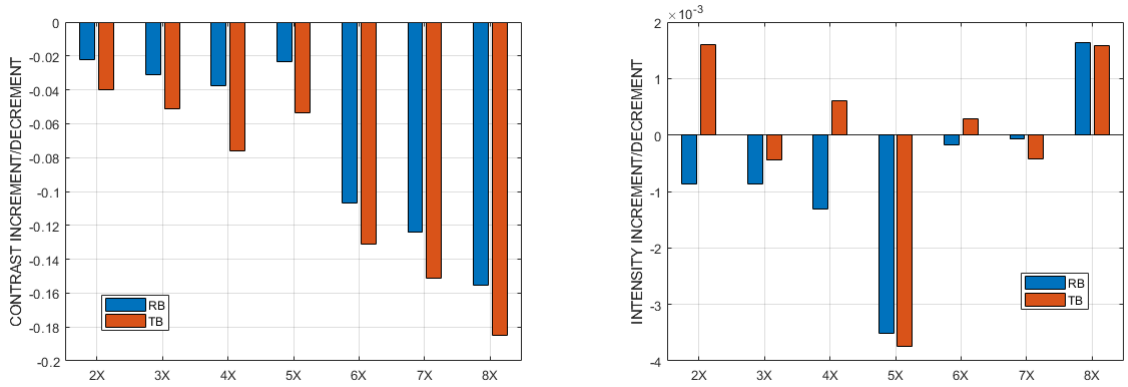


Figure 4: Contrast and Intensity increments or decrements in Lenna images interpolated by TB and RB algorithms.

However, RB algorithm showed a bigger increment only at the interpolation ratio that equals to five. In terms of intensity, the TB algorithm achieved a bigger increment and a smaller decrement than the RB algorithm.

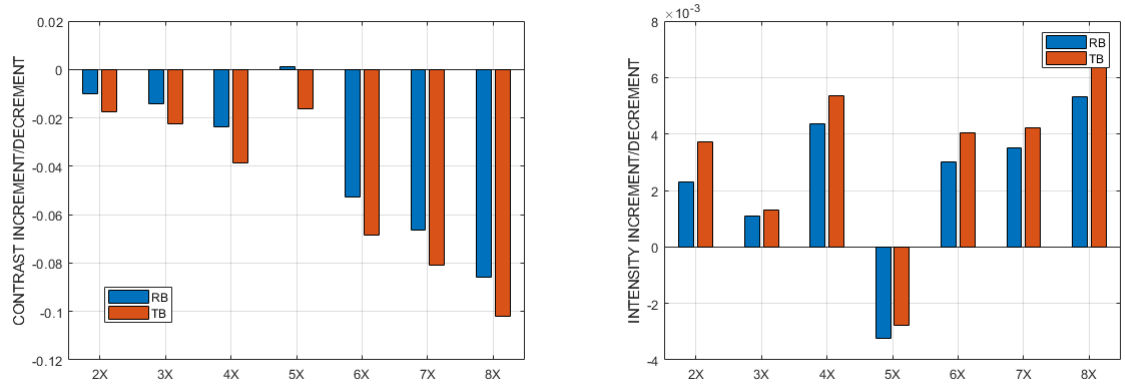


Figure 5: Contrast and Intensity increments or decrements in House images interpolated by TB and RB algorithms.

In Figure 6, the RB algorithm demonstrated a smaller decrement than the TB in terms of contrast at the interpolation ratios used. In terms of intensity, the TB algorithm achieved bigger increment and a smaller decrement than the RB algorithm at the interpolation ratios used.

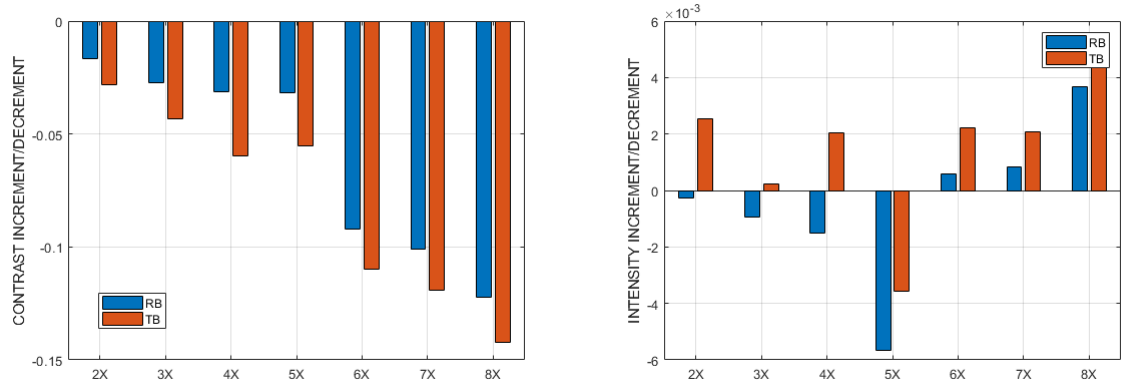


Figure 6: Contrast and Intensity increments or decrements in Cameraman images interpolated by TB and RB algorithms.
Also, in Figure 7, the RB algorithm demonstrated a smaller decrement than the TB in terms of contrast at the interpolation ratios used. In terms of intensity, the TB algorithm achieved bigger increment and a smaller decrement than the RB algorithm at the interpolation ratios used.

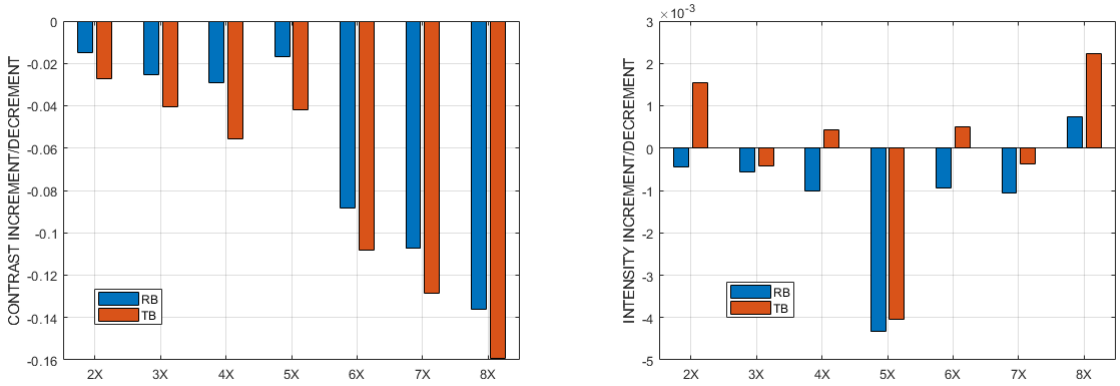


Figure 7: Contrast and Intensity increments or decrements in Peppers images interpolated by TB and RB algorithms.

In Figure 8, the RB algorithm demonstrated a smaller decrement than the TB in terms of contrast at the interpolation ratios used. In terms of intensity, the RB algorithm achieved a bigger increment than the TB algorithm at the interpolation ratios used. In Figure 9, at the interpolation ratio that equals to two, the RB didn't show any increment or decrement in terms of contrast.

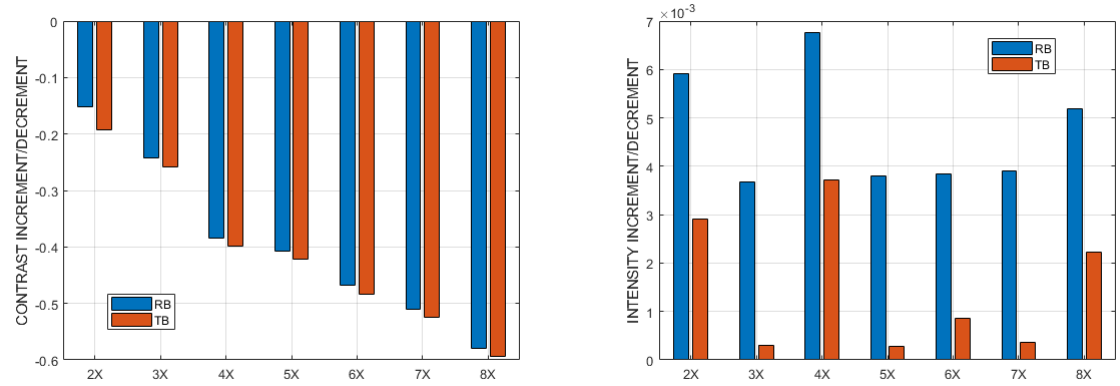


Figure 8: Contrast and Intensity increments or decrements in Aerial images interpolated by TB and RB algorithms.

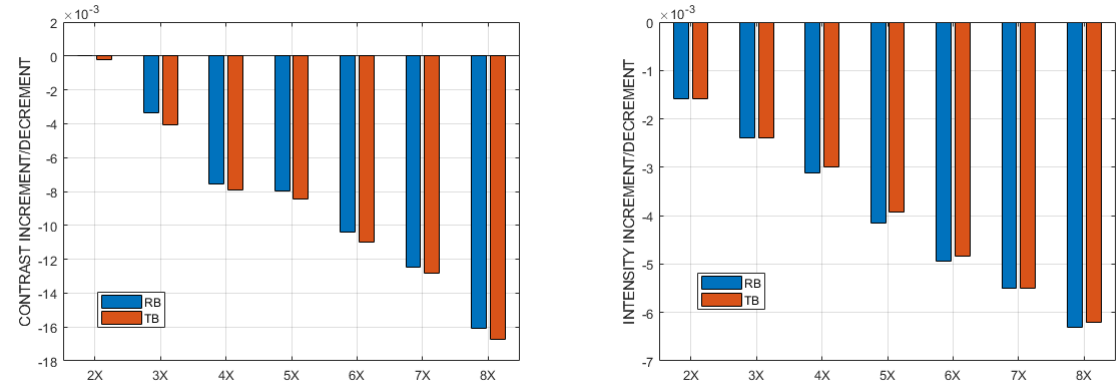


Figure 9: Contrast and Intensity increments or decrements in Gray images interpolated by TB and RB algorithms.
At other interpolation ratios, the RB algorithm demonstrated smaller decrement than the TB in terms of contrast. In terms of intensity, at the interpolation ratio that equals to two, three and seven, both TB and RB algorithms tied. At other interpolation ratios, the TB algorithm demonstrated smaller decrement than the RB algorithm.

Figure 10: Source test grayscale images of the size 170 x 170

The time elapsed performance measurement between the RB and TB demonstrated that the RB algorithm was slower than the TB algorithm. As can be seen in Figure 11, there is a visibly small difference between the images interpolated using the TB and RB algorithms. On top of that, the blurriness artefacts are not to the same extent or level. However, a big difference can be easily be noticed looking at the corresponding small versions, presented in Figure 10. In Figure 12, the edge features among interpolated images (using both algorithms) have almost the same sharpness with a debatable smoothness difference. In Figure 13, we have almost the same situation (looking straight to the edge and texture features) but not the same contrast level in both images. Note that, if the metrics produced the highest or least values, it meant that were more closely related to the corresponding reference images which might or might not match with subjective evaluations.

Figure 11: 3x-interpolated images using the TB algorithm (left) and RB algorithm (right)

Potential applications of the proposed RB method may include ultrasound scan conversion for displaying the sectored image. This possibility is based on the preliminary experiments conducted, using the ultrasound data to display the sectored image, which revealed the reduction in BRISQUE-scored-distortions by 0.4%, 0.42%, 0.63%, as shown in Table 4. Note that three different frames/images data have been used and, the TB's brisque score was used as the reference or original score while the RB's brisque score was used as the targeted score. Here, it is also important to note that to compare the proposed RB method against the TB algorithm because it is meaningful because TB is a commonly used interpolation method for scan conversion [21].

Figure 12: 3x-interpolated images using the TB algorithm (left) and RB algorithm (right)

Figure 13: 3x-interpolated images using the TB algorithm (left) and RB algorithm (right)

Also, it is important to note that in the absence of a reference ultrasound data image, only non-reference metric could be used to estimate increase or decrease in objectively quantifiable distortions.

Table 4: TB and RB brisque scores

| IMAGE 1 | | IMAGE 2 | | IMAGE 3 | |
|---|---|---|---|---|---|
| TB | RB | TB | RB | TB | RB |
| 46.2410 | 46.0568 | 46.9549 | 46.7564 | 46.4631 | 46.1719 |

## 5. CONCLUSION

Effects of interpolating rescaled pixels have been studied in this paper for image interpolation quality. Many works on image interpolation kept focusing on the minimization of visual artefacts by working on the weighting functions which was not the case in this paper since we focused on the effects of rescaling pixels in the spatial domain. Therefore, this paper proposed a solution that used rescaled pixels. The new interval or range (or lower and upper bounds limit) for pixel rescaling purposes was obtained using statistical mean and standard deviation of a vector of four nearest pixels. Effects were investigated using standard full-reference and non-reference quality metrics as well as variance and mean based metrics. Natural image-based experiments demonstrated that the rescaled bilinear interpolation algorithm achieved generally smaller decrements than the traditional bilinear interpolation algorithm in terms of image quality indicators, mentioned. Also, the feature similarities between rescaled and traditional algorithms remained comparable, except in terms of image distortions. This suggests that rescaling image pixels was a non-trivial way to go in optimizing the bilinear interpolation algorithm. The problem with the rescaling scheme was an increase in processing time compared to the traditional method as well as being image type dependent in performance. With the ultrasound scan conversion, the rescaled bilinear algorithm proved to be better than the traditional bilinear algorithm as it showed more image details and fewer distortions in interpolated images. Future research efforts may be put in the development of new strategies that would fasten the interpolation process and that would consider variable kernels in the effort to improve the quality of both natural and sectored images.

## REFERENCES


[1] Burningham, N., Pizlo, Z., Allebach, J. P., "Image Quality Metrics," In Hornak, Joseph P. Encyclopedia of imaging science and technology. New York: Wiley, (2002)

[2] Su, D., Willis, P., "Image interpolation by pixel-level data-dependent triangulation," Computer Graphics Forum, 23(2), pp. 189–201, (2004)

[3] Pan, M., Yang, X., and Tang, J., "Research on interpolation methods in medical image processing," Journal of Medical Systems, 36(2), pp. 777–807, (2010)

[4] Rukundo, O., Cao, H.Q., "Nearest neighbor value interpolation," International Journal of Advanced Computer Science and Applications, 3(4), pp. 25–30, (2012)

[5] Rukundo, O., Cao, H.Q., Huang, M.H., "Optimization of bilinear interpolation based on ant colony algorithm," Lecture Notes in Electrical Engineering 137, Springer Berlin Heidelberg, pp. 571–580, (2012)

[6] Rukundo, O., Maharaj, B.T., "Optimization of image interpolation based on nearest neighbour algorithm," International Conference on Computer Vision Theory and Applications VISAPP, pp. 641–647, (2014)

[7] Rukundo, O., Cao, H.Q., "Advances on image interpolation based on ant colony algorithm," SpringerPlus 5 (1), 403, (2016)

[8] Rukundo, O., "Effects of improved-floor function on the accuracy of bilinear interpolation algorithm," Computer and Information Science, 8(4), pp. 1–11, (2015)

[9] Rukundo, O., Wu, K.N., Cao, H.Q., "Image interpolation based on the pixel value corresponding to the smallest absolute difference," Fourth International Workshop on Advanced Computational Intelligence IWACI, pp. 432–435, (2011)

[10] Luong, H.Q., De Smet, P., Philips, W., "Image interpolation using constrained adaptive contrast enhancement techniques," IEEE International Conference on Image Processing ICIP, pp. 998–1001, (2005)

[11] Rukundo, O., "Half-unit weighted bilinear algorithm for image contrast enhancement in capsule endoscopy," Proc. SPIE 10615, Ninth International Conference on Graphic and Image Processing,106152Q, (2018)

[12] Rukundo, O., "Effects of empty bins on image upscaling in capsule endoscopy," Proc. SPIE 10420, Ninth International Conference on Digital Image Processing, 104202P, (2017)

[13] Rukundo, O., Schmidt, S., "Aliasing artefact index for image interpolation quality assessment," Proc. SPIE 10817, Optoelectronic Imaging and Multimedia Technology V, (2018)

[14] Mittal, A., Moorthy, A. K., Bovik, A. C., "No-reference image quality assessment in the spatial domain," IEEE Transaction on Image Processing 21, pp. 4695–4708, (2012)

[15] Sheikh, H.R., Sabir, M.F., Bovik, A.C., "A statistical evaluation of recent full reference image quality assessment algorithms," IEEE Transactions on Image Processing, 15(11), pp. 3440–3451, (2006)

[16] Zhang, L., Zhang, L., Mou, X., Zhang, D., “FSIM: A feature similarity index for image quality assessment,” IEEE Transactions on Image Processing, 20(8), pp. 2378–2386, (2011)
[17] Wang, Z., Bovik, A.C., Sheikh, H.R., "Image Quality Assessment: From Error Visibility to Structural Similarity", IEEE Transactions on Image Processing, 13(4), pp. 600-612, (2004)
[18] Rukundo, O., Pedersen, M., Hovde, Ø., "Advanced Image Enhancement Method for Distant Vessels and Structures in Capsule Endoscopy," Computational and Mathematical Methods in Medicine, 2017, (2017)
[19] Imtiaz, M.S., Wahid, K. A., “Color enhancement in endoscopic images using adaptive sigmoid function and space variant color reproduction,” Computational and Mathematical Methods in Medicine, vol. 2015, Article ID 607407, (2015)
[20] Rukundo, O., Schmidt, S., "Extrapolation for image interpolation," Proc. SPIE 10817, Optoelectronic Imaging and Multimedia Technology V, (2018)
[21] Li, X.H., "Ultrasound Scan Conversion on TI’s C64x+ DSPs," Application Report SPRAB32, Texas Instruments, March 2009